Applied Mathematical Modelling 52 (2017) 437–457

Contents lists available at ScienceDirect

Applied Mathematical Modelling

journal homepage: www.elsevier.com/locate/apm

Mathematical model for pest–insect control using mating disruption and trapping

Roumen Anguelov[a], Claire Dufourd[a,*], Yves Dumont[b,c]

[a] Department of Mathematics and Applied Mathematics, University of Pretoria, Pretoria, South Africa
[b] CIRAD, UMR AMAP, F-34398 Montpellier, France
[c] AMAP, Univ Montpellier, CIRAD, CNRS, INRA, IRD, Montpellier, France

ARTICLE INFO

Article history:
Received 16 June 2016
Revised 20 July 2017
Accepted 31 July 2017
Available online 7 August 2017

Keywords:
Piecewise-smooth system
Stability analysis
Pest control
Pheromone traps
Mating disruption
Insect trapping

ABSTRACT

Controlling pest insects is a challenge of main importance to preserve crop production. In the context of Integrated Pest Management (IPM) programs, we develop a generic model to study the impact of mating disruption control using an artificial female pheromone to confuse males and adversely affect their mating opportunities. Consequently the reproduction rate is diminished leading to a decline in the population size. For more efficient control, trapping is used to capture the males attracted by the artificial pheromone. The model, derived from biological and ecological assumptions, is governed by a piecewise smooth system of ODEs. A theoretical analysis of the model without control is first carried out to establish the properties of the endemic equilibrium. Then, control is added and the theoretical analysis of the model enables to identify threshold values of pheromone which are practically interesting for field applications. In particular, we show that there is a threshold above which the global asymptotic stability of the trivial equilibrium is ensured, i.e. the population goes to extinction. Finally, we illustrate the theoretical results via numerical experiments.

1. Introduction

Pest insects are responsible for considerable damages on crops all over the world. Their presence can account for high production losses having repercussions on trading and exports as well on the sustainability of small farmers whose incomes entirely rely on their production. Exotic pests, can be particularly harmful as they can exhibit high invading potential due to the lack of natural enemies and their capacity to adapt to wide range of hosts and/or climate conditions. Therefore, pest management is essential to prevent devastating impact on economy, food security, social life, health and biodiversity.

Chemical pesticides have long been used to control pest populations. However, their extensive use can have undesired side effects on the surrounding environment, such as reduction of the pest's natural enemies and pollution. Further, the development of insect resistance to the chemical lead to the need of using stronger and more toxic pesticides to maintain their efficacy. Thus, extensive use of pesticides is not a sustainable solution for pest control. Constant efforts are being made to reduce the toxicity of the pesticides for applicators and consumers, and alternative methods are being developed or improved to satisfy the charter of Integrated Pest Management (IPM) programs [1]. IPM aims to maintain pest population

* Corresponding author.
E-mail address: claire.dufourd@gmail.com (C. Dufourd).

http://dx.doi.org/10.1016/j.apm.2017.07.060
0307-904X/

at low economic and epidemiological risk while respecting specific ecological and toxicological environmentally friendly requirements.

Mating disruption (MD), Sterile Insect Technique (SIT), and Mass Annihilation Technique (MAT) are examples of methods part of IPM strategies. SIT consists in releasing large numbers of sterilized males to compete with wild males for female insemination, reducing the number of viable offspring, while MAT consists in reducing the number of one or both sexes by trapping using a species-specific attractant. MD consists of introducing an artificial stimuli, like pheromones or parapheromones [2,3], to confuse individuals [4] and, thus, disrupt mate localization, leading to long-term reduction of the population [5]. In this paper, we mainly focus on MD, eventually coupled with trapping.

MD has been widely studied and used to control different type of pests on various type of crops. It has shown to be successful for the control of: *Tuta absoluta* on tomato crops in Italian greenhouses [6]; the pink bollworm *Pectinophora gossypiella* which attacks cotton, the apple codling moth *Cydia pomonella* [7]; the California red scale, *Aonidiella aurantii*, and the citrus leafminer, *Phyllocnistis citrella*, in Citrus Orchard [8,9].

However, MD has sometimes been a failure as for the control of the coffee leaf miner *Leucoptera coffeela* [10] or for the control of the tomato pest *Tuta absoluta* mentioned above in open field conditions [11] where mating disruption did not manage to reduce the pest population. According to [10,11], the failure of the method may be attributed to composition and dosage of the pheromone and/or to a high abundance of insects.

For mating disruption success, understanding the attraction mechanisms of the pest to the pheromone is important, like the minimum level response, the distance of attraction or the formulation of the pheromone used. Environmental constrains are also crucial factors to take into account. These include the climate, the wind, the crop's foliage, etc. Further, the population size must be accounted for in order to design appropriate control strategies. Thus, planning efficient and cost effective control is a real challenge which can explain the failure of the experiments mentioned above. Mathematical modeling can be very helpful to get a better understanding on the dynamics of the pest population, and various control strategies can be studied to optimize the control. Here, we combine mating disruption using female-sex pheromone lures to attract males away from females in order to reduce the mating opportunities adversely affecting the rate reproduction. For more efficient control, lures can be placed in traps to reduce the male population.

In this paper, we built a generic model for the control of a pest population using mating disruption and trapping to study the effort required to reduce the population size below harmful level. The model is derived using general knowledge or assumptions on insects' biology and ecology. We consider a compartmental approach based on the life cycle and mating behavior to model the temporal dynamics of the population which is governed by a piecewise smooth (PWS) system of ordinary differential equations [12,13]. A theoretical analysis of the model is carried out to discuss the efficiency of the control using pheromone traps depending on the strength of the lure and the trapping efficacy. The main issue of practical importance is what values of these parameters provide effective control leading to extinction. Equivalently, in mathematical terms, the question is for what values of the parameters the solution of the model converges to the model's trivial equilibrium where all compartments equal zero. We study the properties of the equilibria using the amount of pheromone as a bifurcation parameter. We identify two threshold values of practical importance. One corresponds to the minimum amount of lure required to affect the female population equilibrium, while the second one is the threshold above which extinction of the population is achieved. We also show that on small enough populations, at invasion stage for instance, extinction may be achieved with a small amount of lure. We also show that combining mating disruption with trapping significantly reduces the amount of pheromone needed to obtain a full control of the population. Let us mention that MD control has been considered in [14–16] using discrete density-dependent models. In the later, the authors identified a threshold value for the amount of pheromone above which the control of an insect population is possible.

The paper is organized as follows. In Section 2, we give a description of the model without control and analyze it theoretically. Then, in Section 3, we describe the model with MD and provide a theoretical analysis, where we identify two threshold values which determine changes in the dynamics of the pest population and the control efficiency. In Section 4, we perform numerical simulations to illustrate the theoretical results and discuss their biological relevance. Finally, in Section 5, we conclude and discuss possible perspectives and extensions.

2. Mathematical modeling of natural insect population

2.1. Compartmental model of the insect population

We consider a generic model to describe the dynamics of a pest insect population based on biological and behavioral assumptions. For many pest species, such as fruit flies or moths, two main development stages can be considered: the immature stage, denoted I, which gathers eggs, larvae and pupae, and the adult stage. Typically, the adult female is the one responsible for causing direct damage to the host when laying her eggs. We split the adult females in two compartments, the females available for mating denoted Y, and the fertilized females denoted F. We assume that a mating female needs to mate with a male in order to pass into the compartment of the fertilized females and be able to deposit her eggs. Therefore, we also add a male compartment, denoted M, to study how the abundance of males impacts the transfer rate from Y to F. We make the model sufficiently generic such that multiple mating can occur, which implies that fertilized females can become mating female again.

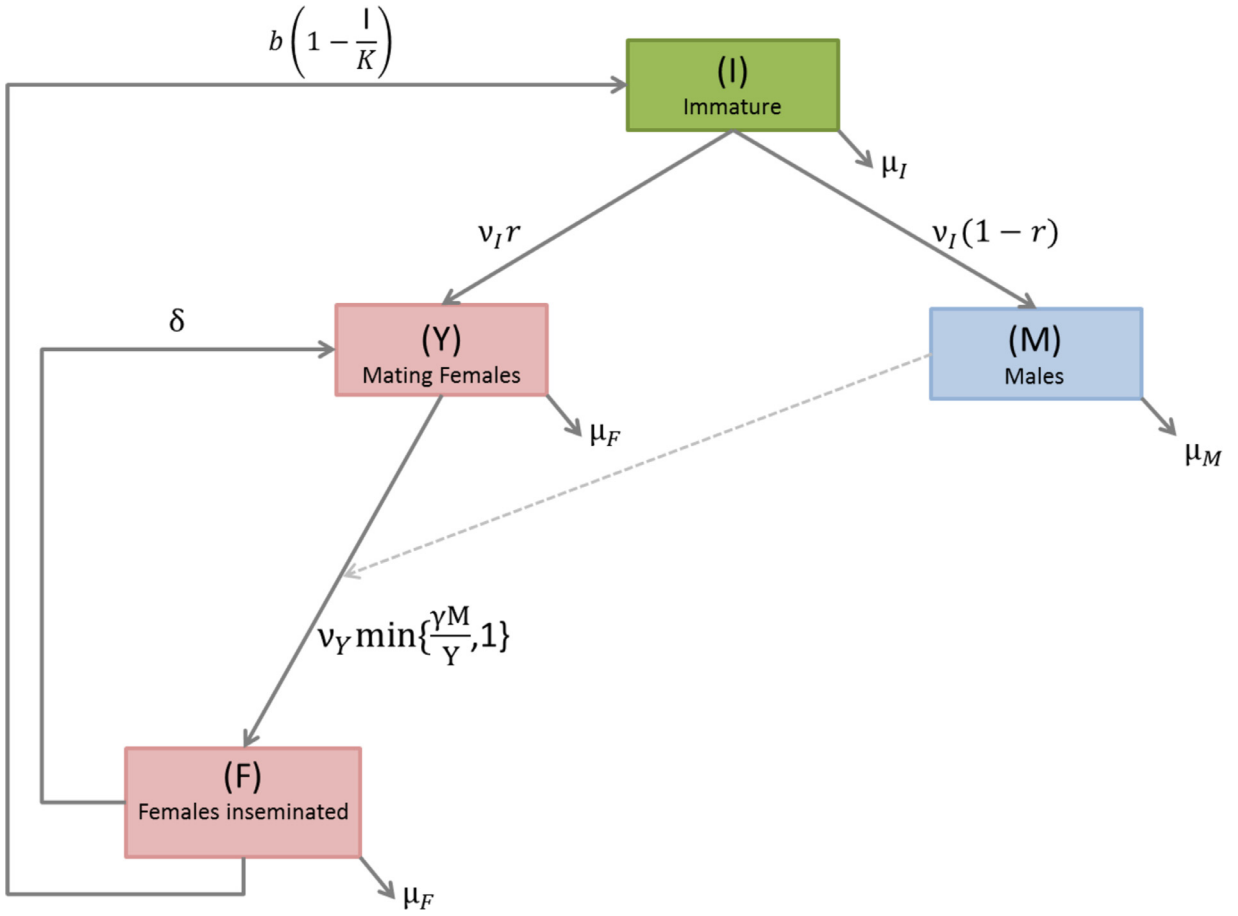

Fig. 1. Life cycle of the insect.

We denote r the proportion of females emerging from the immature stage and entering the mating females compartment. Thus a proportion of $(1-r)$ on the immature enter the male compartment after emergence. We assume that the time needed for an egg laid to emergence is $1/\nu_I$, thus the transfer rate from I to Y or M is ν_I. Then, when males are in sufficient abundance to ensure the fertilization of all the females available for mating, the transfer rate from Y to F is ν_Y. However, if males are scarce, and if γ is the number of females that can be fertilized by a single male, then only a proportion $\frac{\gamma M}{Y}$ of Y-females can pass into the F-females compartment. Therefore, the transfer rate from Y to F is modeled by the non-linear term $\nu_Y \min\{\frac{\gamma M}{Y}, 1\}$. Moreover, fertilized females go back to the mating females compartment with a rate of δ. Further, the fertilized females supply the immature compartment with a rate $b\left(1-\frac{I}{K}\right)$, where b is the intrinsic egg laying rate, while K is the carrying capacity of the hosts. Finally, parameters μ_I, μ_F, μ_M are respectively the death rates of immatures (compartment I), females (Y and F) and males (M). The flow diagram of the insects' dynamics is represented in Fig. 1.

The model is governed by the following system of ODEs:

$$\begin{cases} \frac{dI}{dt} = b\left(1-\frac{I}{K}\right)F - (\nu_I + \mu_I)I, \\ \frac{dY}{dt} = r\nu_I I - \nu_Y \min\{\frac{\gamma M}{Y}, 1\}Y + \delta F - \mu_F Y, \\ \frac{dF}{dt} = \nu_Y \min\{\frac{\gamma M}{Y}, 1\}Y - \delta F - \mu_F F, \\ \frac{dM}{dt} = (1-r)\nu_I I - \mu_M M. \end{cases} \tag{1}$$

The list of the parameters used in the model are summarized in Table 1. They are taken from [17] in order to perform numerical experiments.

More precisely, (1) can be written in the form

$$\frac{dx}{dt} = f(x) := \begin{cases} f_1(x) & \text{if} \quad Y \le \gamma M \\ f_2(x) & \text{if} \quad Y \ge \gamma M \end{cases}, \tag{2}$$

Table 1
List of parameters and there values used in the numerical simulations.

Parameter	Description	Unit	Value
b	Intrinsic egg laying rate	$\text{Female}^{-1}\text{day}^{-1}$	9.272
r	Female to male ratio	–	0.57
K	Carrying capacity	–	1000
γ	Females fertilized by a single male	–	4
μ_I	Mortality rate in the I compartment	Day^{-1}	1/15
μ_F	Mortality rate in the Y and F compartments	Day^{-1}	1/75.1
μ_M	Mortality rate in the M compartment	Day^{-1}	1/86.4
ν_I	Transfer rate from I to Y	Day^{-1}	1/24.6
ν_Y	Transfer rate from Y to F	Day^{-1}	0.5
δ	Transfer rate from F to Y	Day^{-1}	0.1

where $x = (I, Y, F, M)^T \in \mathbb{R}^4_+$ and

$$f_1(x) = \begin{pmatrix} b\left(1-\frac{I}{K}\right)F - (\nu_I + \mu_I)I \\ r\nu_I I + \delta F - (\nu_Y + \mu_F)Y \\ \nu_Y Y - (\delta + \mu_F)F \\ (1-r)\nu_I I - \mu_M M \end{pmatrix}, \quad f_2(x) = \begin{pmatrix} b\left(1-\frac{I}{K}\right)F - (\nu_I + \mu_I)I \\ r\nu_I I + \delta F - \nu_Y \gamma M - \mu_F Y \\ \nu_Y \gamma M - (\delta + \mu_F)F \\ (1-r)\nu_I I - \mu_M M Piecewise - smooth \end{pmatrix}. \tag{3}$$

Considering the context of the model (1), we refer to the region defined via $Y < \gamma M$ as a *male abundance region* and the region defined via $Y > \gamma M$ as *male scarcity region* with the respective systems given via

$$\frac{dx}{dt} = f_1(x) \tag{4}$$

and

$$\frac{dx}{dt} = f_2(x). \tag{5}$$

Both (4) and (5) are usual systems of ODEs with smooth right-hand side. Their properties can be investigated using standard techniques for such systems. However, deriving the properties of (1) is not a straight-forward process. It generally belongs to the theory of piecewise-smooth dynamical systems. In the next section, we provide some basics of this theory which are relevant to deriving the results in this paper. See also [12,13] for a complete overview.

2.2. Piecewise-smooth dynamical systems

Definition 1 ([12], Definition 2.2.2, p. 73)**.** A piecewise-smooth flow is given by a finite set of ODEs

$$\dot{x} = F_i(x, \mu), \qquad x \in S_i,$$

where $\cup_i S_i = \mathcal{D} \subset \mathbb{R}^n$, each S_i has a non-empty interior, and $\mathcal{D}$ is a domain. The intersection $\sum_{ij} := \overline{S}_i \cap \overline{S}_j$ is either an $\mathbb{R}^{n-1}$-dimensional manifold included in the boundaries ∂S_j and ∂S_i, or is the empty set. Each vector field F_i is smooth in both state x and parameter μ, and defines a smooth flow $\Phi_i(x, t)$ within any open set $U \supset S_i$. In particular, each flow Φ_i is well defined on both side of the boundary ∂S_i.

A non-empty border between two regions Σ_{ij} will be called a discontinuity set, discontinuity boundary, or a switching manifold.

In the rest of the paper, we will mainly consider the following system with a single discontinuity set $\sum = \sum_{12}$:

$$\dot{x} = \begin{cases} F_1(x, \mu), & \text{if } x \in S_1 \\ F_2(x, \mu), & \text{if } x \in S_2 \end{cases}, \tag{6}$$

where $S_1 \cup S_2 = \mathcal{D}$, F_1 generates a flow Φ_1, F_2 a flow Φ_2. When $F_1(x) = F_2(x)$ at a point $x \in \Sigma$, but there is a difference in the Jacobian derivatives $F_{1,x} \neq F_{2,x}$ at x, then the degree of smoothness is said to be 2.

Definition 2. Systems with smoothness of degree 2 or higher are called *piecewise-smooth continuous systems* (PWCS).

In fact according to the following general definition

Definition 3 ([13], Definition 2.1, p. 638)**.** A discontinuity boundary Σ is said to be uniformly discontinuous in some domain $\mathcal{D}$ if the degree of smoothness of the vector field across Σ is the same throughout $\mathcal{D}$. Furthermore, we say that the discontinuity is uniform with degree $m+1$ if the first $m-1$ derivatives of $F_1 - F_2$, evaluated on Σ, are zero.

the switching manifold Σ is uniform with degree of smoothness 2. Let us consider that system (6) rewritten as follows

$$\dot{x} = \begin{cases} F_1(x,\mu), & \text{if } H(x,\mu) > 0 \\ F_2(x,\mu), & \text{if } H(x,\mu) < 0 \end{cases}, \tag{7}$$

where H defines the switching manifold Σ by

$$\sum := \{x \in \mathcal{D} : H(x) = 0\}.$$

For PWCS system (7), it is possible to identify different types of equilibria, leading to the following definition

Definition 4 ([13], Definition 2.2, p. 640)**.** We term a point $x \in \mathcal{D}$ as a *regular equilibrium* of (7) if x is such that either

$$F_1(x,\mu) = 0 \text{ and } H(x,\mu) > 0$$

or

$$F_2(x,\mu) = 0 \text{ and } H(x,\mu) < 0.$$

Alternatively, we say that a point $y \in \mathbb{D}$ is a *virtual equilibrium* of (7) if either

$$F_1(y,\mu) = 0 \text{ and } H(y,\mu) < 0$$

or

$$F_2(y,\mu) = 0 \text{ and } H(y,\mu) > 0.$$

For standard autonomous continuous system, i.e. $\dot{x} = f(x)$, with $f : G^* \to \mathbb{R}^n$ continuous, and G^* an open set in $\mathbb{R}^n$, according to well known theory, for any given initial conditions $x_0 \in G^*$, we have existence of a unique solution $u(t, x_0)$. Let also V a compact set in $\mathbb{R}^n$. Then to study the local or global asymptotically stability of equilibria, we consider the following general definitions

Definition 5 ([18], Definition 7.1, p. 32)**.** A compact set $V \subset G^*$ is said to be *stable*, if given a neighborhood U of V, there is a neighborhood W of V such that $x \in W$ implies $u(t, x) \in U$ for all $t \geq 0$.

Definition 6 ([18], Definition 7.5, p. 32)**.** A compact set $V \subset G^*$ is an attractor if there is a neighborhood U of V such that $x \in U$ implies $u(t, x) \to V$ as $t \to \infty$. If $u(t, x) \to V$ for each $x \in G^*$, V is called a *global attractor*. If V is both stable and an attractor, V is said to be *asymptotically stable*. V is said to be *globally asymptotically stable* if it is stable and a global attractor.

2.3. Theoretical analysis of the model

The theoretical analysis of the model is carried out by considering (2) as a PWS system, on $\mathbb{R}^4_+$. Here the switching manifold is $\Sigma = \{x \in \mathbb{R}^4_+ : Y = \gamma M\}$. Since we have that $f_1(x) = f_2(x)$, $x \in \Sigma$, (2) is a PWCS system. The derivatives of f_1 and f_2 exist on Σ, but, in general, they are not equal. In terms of the previous terminology for PWS systems, the discontinuity across Σ is uniform with degree of smoothness equal to 2. For this special type of systems the local existence and uniqueness of solutions follows from the standard ODE theory since f is Lipschitz, which is the minimum required. Further, it is easy to see that the system (2) is dissipative, which provides for global existence of the solutions on the time interval $[0, +\infty)$.

First, we will study the systems (4) and (5) separately and then the obtained results will be merged into a theorem for the system (1). According to Definition 4, in our setting, a point $\bar{x} = (\bar{I}, \bar{Y}, \bar{F}, \bar{M})^T$ is called a *virtual equilibrium* of (2) if $f_1(\bar{x}) = 0$, $\bar{Y} > \gamma \bar{M}$ or $f_2(\bar{x}) = 0$, $\bar{Y} < \gamma \bar{M}$.

2.3.1. Case 1: male abundance

The analysis of (4) uses the theory of cooperative systems [19].

An autonomous system of ODEs

$$\frac{dx}{dt} = \Psi(x) \tag{8}$$

where $\Psi : D \longrightarrow \mathbb{R}^n$, $x \in D \subset \mathbb{R}^n$, is called cooperative if Ψ_i is monotone increasing with respect to x_j, $i, j = 1, \ldots, n$, $j \neq i$. A function Ψ with the stated monotonicity is called quasi-monotone.

For reader's convenience, we recall two main theorems that we will use in the rest of the paper:

Theorem 7. *[19, Theorem 3.1, p. 18], [20, Theorem 6] Let $a, b \in D$, such that $a \leq b$, $[a, b] \subseteq D$ and $f(b) \leq \mathbf{0} \leq f(a)$. Then (8) defines a positive dynamical system on $[a, b]$. Moreover, if $[a, b]$ contains a unique equilibrium p then, p is globally asymptotically stable (GAS) on $[a, b]$.*

Theorem 8. *Let $a, b \in D$, such that $a \leq b$, $[a, b] \subseteq D$ and $f(a) = f(b) = 0$ for (8). Then*

(a) *(8) defines a positive dynamical system on $[a, b]$.*

(b) *If a and b are the only equilibria of the dynamical system on* $[a, b]$, *then all solutions initiated in the interior of* $[a, b]$ *converge to one of them, that is, either all converge to a or all converge to b.*

The persistence of a population is typically linked to its basic offspring number. For simple population models the basic offspring number is defined as the number of offspring produced by a single individual in their life time provided abundant resource is available. In general, the definition could be more complicated and its value is computed by using the next generation method. For the model in (4), straightforward computations leads to the following basic offspring number

$$\mathcal{N}_0 = \frac{br\nu_I\nu_Y}{(\mu_I+\nu_I)((\nu_Y+\mu_F)(\delta+\mu_F)-\delta\nu_Y)}. \tag{9}$$

In this paper we will use $\mathcal{N}_0$ only as a threshold parameter. The persistence when $\mathcal{N}_0 > 1$ and the extinction when $\mathcal{N}_0 < 1$ are given direct proofs. Hence, we will not discuss the details on specific properties of the number. The persistence or extinction of a population are typically represented in a model setting via the concept of *global asymptotic stability* of the endemic or trivial (zero) equilibrium, respectively.

Theorem 9.

(a) *The system of ODE (4) defines a positive dynamical system on* $\mathbb{R}^4_+$.
(b) *If* $\mathcal{N}_0 \le 1$ *then* $TE = (0,0,0,0)^T$ *is a globally asymptotically stable (GAS) equilibrium.*
(c) *If* $\mathcal{N}_0 > 1$ *then TE is an unstable equilibrium and the system admits a positive equilibrium* $EE^* = (I^*, Y^*, F^*, M^*)^T$, *where*

$$\begin{aligned}
I^* &= \left(1-\frac{1}{\mathcal{N}_0}\right)K,\\
Y^* &= \frac{r\nu_I(\delta+\mu_F)}{(\nu_Y+\mu_F)(\delta+\mu_F)-\delta\nu_Y}\left(1-\frac{1}{\mathcal{N}_0}\right)K,\\
F^* &= \frac{r\nu_I\nu_Y}{(\nu_Y+\mu_F)(\delta+\mu_F)-\delta\nu_Y}\left(1-\frac{1}{\mathcal{N}_0}\right)K,\\
M^* &= \frac{(1-r)\nu_I}{\mu_M}\left(1-\frac{1}{\mathcal{N}_0}\right)K,
\end{aligned}$$

which is a globally asymptotically stable (GAS) on $\mathbb{R}^4_+ \setminus \{x \in \mathbb{R}^4_+ : I = Y = F = 0\}$.

Proof. Solving $f_1(x) = 0$ yields two solutions *TE* and EE^*, where $EE^* > 0$ iff $\mathcal{N}_0 > 1$. The properties of existence of solutions and assymptotic stability properties of equilibria *TE* and EE^* are established via standard methods of analysis of systems of ODEs. We derive here the proof of the global attractiveness of the equilibria which uses a not very common approach based on the theory of cooperative systems. It is easy to see that (4) is cooperative on $\Omega_K = \{x \in \mathbb{R}^4_+ : I \le K\}$ because f_1 is quasimonote on Ω_K.

Let $q \in \mathbb{R}$, $q \ge K$. Denote

$$y_q = \begin{pmatrix} K \\ \frac{r\nu_I(\delta+\mu_F)}{(\nu_Y+\mu_F)(\delta+\mu_F)-\delta\nu_Y}q \\ \frac{r\nu_I\nu_Y}{(\nu_Y+\mu_F)(\delta+\mu_F)-\delta\nu_Y}q \\ \frac{(1-r)\nu_I}{\mu_M}q \end{pmatrix} \tag{10}$$

We have $f_1(\mathbf{0}) = \mathbf{0}$ and $f_1(y_q) \le \mathbf{0}$. Then, from Theorem 7 it follows that (4) defines a positive dynamical system on $[\mathbf{0}, y_q]$.

Let $\mathcal{N}_0 \le 1$ (point b). In this case *TE* is the only equilibrium on $[\mathbf{0}, y_q]$ and it follows from Theorem 7 that it is GAS on $[\mathbf{0}, y_q]$. Hence, TE is also GAS on $\cup_{q\ge K}[\mathbf{0}, y_q] = \Omega_K$.

Let $\mathcal{N}_0 > 1$ (point c). First, using the same approach as for (b) we obtain that EE^* is GAS on $\{x \in \mathbb{R}^4_+ : x \ge EE^*\}$. Secondly, we consider Theorem 8 applied to the interval [*TE*, EE^*]. Since for $\mathcal{N}_0 > 1$ the equilibrium *TE* is not asymptotically stable, the theorem implies that EE^* attracts all solutions in the interior of the interval. Putting the two results together we obtain that EE^* is GAS on the interior of $\mathbb{R}^4_+$. The asymptotic behavior of the solutions on the boundary of $\mathbb{R}^4_+$ can be verified directly to obtain the GAS property of EE^* in (c). □

2.3.2. Case 2: male scarcity

Next we consider the system (5). It is easy to see that the second equation can be decoupled. The system of the remaining three equations is of the form

$$\frac{du}{dt} = g(u), \tag{11}$$

where $u = \begin{pmatrix} I \\ F \\ M \end{pmatrix}$ and $g(u) = \begin{pmatrix} b\left(1-\frac{I}{K}\right)F - (\nu_I+\mu_I)I \\ \nu_Y\gamma M - (\delta+\mu_F)F \\ (1-r)\nu_I I - \mu_M M \end{pmatrix}$.

The basic offspring number for system (11) is

$$\hat{\mathcal{N}}_0 = \frac{b\gamma(1-r)\nu_I\nu_Y}{(\nu_I+\mu_I)(\delta+\mu_F)\mu_M}. \tag{12}$$

The following theorem describes the properties of system (11).

Theorem 10.

(a) *The system of ODE (11) defines a positive dynamical system on* $\mathbb{R}^3_+$.
(b) *If* $\hat{\mathcal{N}}_0 \leq 1$ *then* $TE_3 = (0,0,0)^T$ *is a GAS equilibrium.*
(c) *If* $\hat{\mathcal{N}}_0 > 1$ *then* TE_3 *is an unstable equilibrium and the system admits a positive equilibrium* $\widehat{EE}_3 = (\hat{I},\hat{F},\hat{M})$, *where*

$$\hat{I} = \left(1-\frac{1}{\hat{\mathcal{N}}_0}\right)K,$$

$$\hat{F} = \frac{\gamma(1-r)\nu_I\nu_Y}{(\delta+\mu_F)\mu_M}\left(1-\frac{1}{\hat{\mathcal{N}}_0}\right)K,$$

$$\hat{M} = \frac{(1-r)\nu_I}{\mu_M}\left(1-\frac{1}{\hat{\mathcal{N}}_0}\right)K,$$

which is GAS on $\mathbb{R}^3_+ \setminus \{TE_3\}$.

Using that function g is quasi-monotone and hence, the system (11) is cooperative on $\hat{\Omega}_K = \{x \in \mathbb{R}^3_+ : I \leq K\}$, the global attractiveness properties stated in the Theorem 10 are proved using the same method as in Theorem 9.

It can be deduced from Theorem 10 that the non-trivial equilibrium value of Y is

$$\hat{Y} = \frac{r\nu_I(\delta+\mu_F)\mu_M - \nu_Y\gamma(1-r)\nu_I\mu_F}{\mu_F(\delta+\mu_F)\mu_M}\left(1-\frac{1}{\hat{\mathcal{N}}_0}\right)K. \tag{13}$$

We note that the value of $\hat{Y}$ and in general the value of the variable Y can be negative. Hence, we have the following corollary.

Corollary 11.

(a) *The system of ODE (5) defines a positive dynamical system on* $\mathbb{R}_+ \times \mathbb{R} \times \mathbb{R}^2_+$.
(b) *If* $\hat{\mathcal{N}}_0 \leq 1$ *then* $TE = (0,0,0,0)^T$ *is a GAS equilibrium.*
(c) *If* $\hat{\mathcal{N}}_0 > 1$ *then TE is an unstable equilibrium and* $\widehat{EE} = (\hat{I},\hat{Y},\hat{F},\hat{M})$ *is a positive equilibrium, which is GAS on* $\mathbb{R}_+ \times \mathbb{R} \times \mathbb{R}^2_+ \setminus \{x \in \mathbb{R}^4_+ : I = F = M = 0\}$.

2.3.3. Conclusions for model (1)

In what follows we assume that the population has an endemic equilibrium. Otherwise, no control would be necessary. Further, it is natural to assume that, at equilibrium, there is abundance of males. In terms of the parameters of the model these assumptions can be written as:

$$1.\ \mathcal{N}_0 > 1, \tag{14}$$

$$2.\ Y^* < \gamma M^*. \tag{15}$$

Under the assumptions (14) and (15) we have that $\widehat{EE} > 0$ and $\hat{Y} < \gamma\hat{M}$. Indeed, when $\mathcal{N}_0 > 1$, the inequality

$$\frac{\hat{\mathcal{N}}_0}{\mathcal{N}_0} > 1$$

is equivalent to

$$\gamma > \frac{r(\delta+\mu_F)\mu_M}{(1-r)((\nu_Y+\mu_F)(\delta+\mu_F)-\delta\nu_Y)},$$

which is ensured by (15). Therefore under assumptions (14) and (15) we have that $\hat{\mathcal{N}}_0 > 1$, and by Theorem 10, we have that the system (5) has a non-trivial equilibrium $\widehat{EE}$, which is GAS on $\mathbb{R}_+ \times \mathbb{R} \times \mathbb{R}^2_+ \setminus \{(I,Y,F,M)^T : I = F = M = 0\}$.

Further, under (15), we have

$$\hat{Y} - \gamma\hat{M} = \hat{I}\left(\frac{r\nu_I(\delta+\mu_F)\mu_M - \nu_Y\gamma(1-r)\nu_I\mu_F}{\mu_F(\delta+\mu_F)\mu_M} - \gamma\frac{(1-r)\nu_I}{\mu_M}\right)$$

$$= \frac{\nu_I\hat{I}}{\mu_M}\left(\frac{r\mu_M}{\mu_F} - \gamma(1-r)\frac{\nu_Y\mu_F + \mu_F(\delta+\mu_F)}{\mu_F(\mu_F+\delta)}\right)$$

$$< \frac{\nu_I \hat{I}}{\mu_M}\left(\frac{r\mu_M}{\mu_F} - \frac{r(\delta+\mu_F)\mu_M}{((\nu_Y+\mu_F)(\delta+\mu_F)-\delta\nu_Y)}\frac{\nu_Y\mu_F+\mu_F(\delta+\mu_F)}{\mu_F(\delta+\mu_F)}\right)$$

$$< \frac{\nu_I \hat{I}}{\mu_M}\left(\frac{r\mu_M}{\mu_F} - \frac{r\mu_M}{\mu_F}\right) = 0.$$

To summarize, under assumptions (14) and (15), the globally asymptotically stable equilibria EE^* and $\widehat{EE}$ of (4) and (5), respectively, are in the male abundance region defined via $Y < \gamma M$. Therefore, EE^* is a regular equilibrium of (1), while $\widehat{EE}$ is a virtual one. Moreover, we have the following theorem

Theorem 12. *Given (14) and (15), the model (1) defines a positive dynamical system on $\mathbb{R}^4_+$ and has two equilibria in this domain:*

(a) *TE, which is unstable, and*
(b) *EE^*, which is GAS on $\mathbb{R}^4_+ \setminus \{(I,Y,F,M)^T \in \mathbb{R}^4_+ : I=Y=F=0 \text{ or } I=F=M=0\}$.*

Proof. The fact that (1) defines a dynamical system on $\mathbb{R}^4_+$ as well as the local properties of TE and EE^* follow from Theorem 9, Theorem 10 and the discussion preceding Theorem 12. It remains to prove that EE^* is GAS as stated in (b). The equilibrium EE^* attracts solutions which are entirely in the male abundance region, excluding the M-axis. Solutions in the male scarcity region are attracted to $\widehat{EE} = (\hat{I},\hat{Y},\hat{F},\hat{M})^T$. Hence they leave the male scarcity region and enter the male abundance region. In the male abundance region they are governed by (4) and, therefore, attracted to EE^*. In general this reasoning does not exclude the possibility that a solution may leave the male abundance region, enter the male scarcity region and then leave it. Therefore, we will prove the GAS property of EE^* using a different approach. We consider the system (1) under the transformation

$$(I,Y,F,M)^T \longrightarrow (I,W,F,M)^T, \tag{16}$$

where $W = F + Y$. We obtain the new system

$$\begin{cases} \dfrac{dI}{dt} = b\left(1-\frac{I}{K}\right)F - (\nu_I+\mu_I)I, \\ \dfrac{dW}{dt} = r\nu_I I - \mu_F W, \\ \dfrac{dF}{dt} = \nu_Y \min\{\gamma M,\ W-F\} - \delta F - \mu_F F, \\ \dfrac{dM}{dt} = (1-r)\nu_I I - (\mu_M)M. \end{cases} \tag{17}$$

Since (17) is obtained from (1) via linear transformation, the system (17) defines a positive dynamical system on $\tilde{\Omega} = \{(I,W,F,M)^T \in \mathbb{R}^4_+ : W \geq F\}$ with equilibria the origin and $\widetilde{EE}^* = (I^*,W^*,F^*,M^*)$, where $W^* = Y^* + M^*$. Formulating of the model in the form of (17) is useful because (17) is a cooperative system. Let g denote the right-hand side of (17). It is easy to see that g is quasi-monotone on the considered domain $\tilde{\Omega}$. Then the GAS property of $\widetilde{EE}^*$ is obtained using the method in the proof of Theorem 9 using the point $\tilde{y}_q$ which the image of y_q under the transformation (16). □

3. Modeling mating disruption and trapping

3.1. Mating disruption and trapping

In order to maintain the pest population to a low level, we consider a control using female-pheromone-traps to disrupt male mating behavior. More precisely, we take into account two aspects for the control. The first aspect consists of disturbing the mating between males and females to reduce the fertilization opportunities, which in turn, reduces the number of offspring. This is done using traps that are releasing a female pheromone lure to which males are attracted. This leads to a reduction in the number of males available for mating near the females, and decreases the opportunity for fertilization. The efficiency of mating disruption depends on the strength of the lure or on the number of traps in an area. The second aspect of the control is the trapping potential of the trap. We assume that the lure traps also contain an insecticide which can kill the captured insects.

3.2. The model

In order to take in account the effect of the lures, we consider the approach proposed by Barclay and Van den Driessche [14], and Barclay and Hendrichs [21]. That is, the strength of the lure is represented as the quantity of pheromones released by an equivalent number of wild females. Thus, in the model the effect of the lure corresponds to the attraction of Y_P additional females. In such a setting, the total number of "females" attracting males is $Y + Y_P$ [14]. In particular, this means that males have a probability of $\frac{Y}{Y+Y_P}$ to be attracted to wild females, and a probability of $\frac{Y_P}{Y+Y_P}$ to be attracted

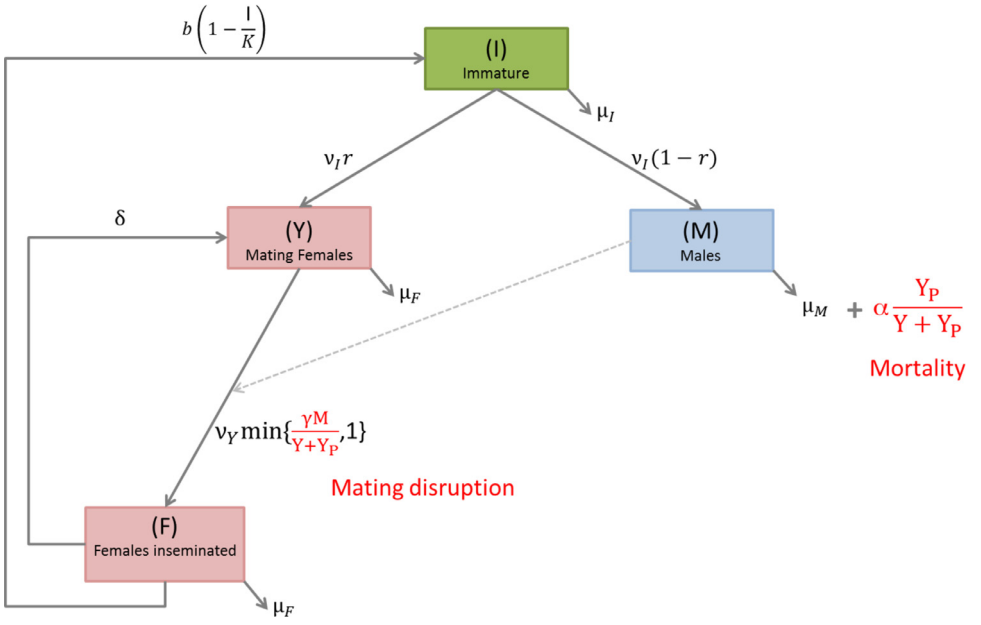

Fig. 2. Control model using mating disruption and trapping.

to the pheromone traps. Denote γ the number of females that can be inseminated by a single male. Then, the transfer rate from Y to F does not exceed $\nu_Y \frac{\gamma M}{Y+Y_P}$. When $\frac{\gamma M}{Y+Y_P} > 1$ the population is in a male abundance state and the transfer rate is ν_Y. However, when $\frac{\gamma M}{Y+Y_P} < 1$, then the population is in a male scarcity state and the transfer rate is $\nu_Y \frac{\gamma M}{Y+Y_P}$. Altogether, the transfer rate is $\nu_Y \min\{\frac{\gamma M}{Y+Y_P}, 1\}$.

The parameter α represents the death or capture rate for the fraction $\frac{Y_P}{Y+Y_P}$ of the males which are attracted by the lures. The flow diagram is represented in Fig. 2 which yields the following system of ODEs:

$$\begin{cases} \frac{dI}{dt} = b\left(1-\frac{I}{K}\right)F - (\nu_I+\mu_I)I, \\ \frac{dY}{dt} = r\nu_I I - \nu_Y \min\{\frac{\gamma M}{Y+Y_P}, 1\}Y + \delta F - \mu_F Y, \\ \frac{dF}{dt} = \nu_Y \min\{\frac{\gamma M}{Y+Y_P}, 1\}Y - \delta F - \mu_F F, \\ \frac{dM}{dt} = (1-r)\nu_I I - (\mu_M + \alpha\frac{Y_P}{Y+Y_P})M. \end{cases} \tag{18}$$

3.3. Theoretical analysis of the control model

Model (18) is a PWS system, where the switching manifold $\Sigma(Y_P) = \{\mathbb{R}^4_+ : Y + Y_P = \gamma M\}$. Similar to (2), it can be written in the form

$$\frac{dx}{dt} = g(x, Y_P) := \begin{cases} g_1(x, Y_P) & \text{if} \quad Y + Y_P \le \gamma M \\ g_2(x, Y_P) & \text{if} \quad Y + Y_P \ge \gamma M \end{cases} \tag{19}$$

where $x = (I, Y, F, M)^T$ and

$$g_1(x, Y_P) = \begin{pmatrix} b\left(1-\frac{I}{K}\right)F - (\nu_I+\mu_I)I \\ r\nu_I I + \delta F - (\nu_Y+\mu_F)Y \\ \nu_Y Y - (\delta+\mu_F)F \\ (1-r)\nu_I I - (\mu_M + \alpha\frac{Y_P}{Y+Y_P})M \end{pmatrix}, \quad g_2(x, Y_P) = \begin{pmatrix} b\left(1-\frac{I}{K}\right)F - (\nu_I+\mu_I)I \\ r\nu_I I + \delta F - \nu_Y\frac{\gamma MY}{Y+Y_P} - \mu_F Y \\ \nu_Y\frac{\gamma MY}{Y+Y_P} - (\delta+\mu_F)F \\ (1-r)\nu_I I - (\mu_M + \alpha\frac{Y_P}{Y+Y_P})M \end{pmatrix} \tag{20}$$

Similarly to (2), the system (19) is a PWS continuous system The existence of solutions follows as for (2). Let us note that the *male abundance region* $\{x \in \mathbb{R}^4_+ : Y + Y_P < \gamma M\}$ and the *male scarcity region* $\{x \in \mathbb{R}^4_+ : Y + Y_P > \gamma M\}$ depend on the control parameter Y_P. As Y_P increases the male abundance region is reduced while the male scarcity region is enlarged. As

in Section 2, we study the properties of the systems associated with male abundance and male scarcity separately and then we draw conclusions for (18).

3.3.1. Case 1: male abundance

The dynamics of the population in the male abundance region $Y + Y_P < \gamma M$ are governed by the following system of ODEs:

$$\begin{cases} \dfrac{dI}{dt} = b\left(1 - \frac{I}{K}\right)F - (\nu_I + \mu_I)I, \\ \dfrac{dY}{dt} = r\nu_I I - \nu_Y Y + \delta F - \mu_F Y, \\ \dfrac{dF}{dt} = \nu_Y Y - (\delta + \mu_F)F, \\ \dfrac{dM}{dt} = (1-r)\nu_I I - (\mu_M + \alpha \frac{Y_P}{Y+Y_P})M. \end{cases} \tag{21}$$

We note that the first three equations in (21) are the same as in (4), while the fourth equation in both systems can be decoupled. Then, using exactly the same method as in Theorem 9 we obtain the following theorem.

Theorem 13.

(a) *The system of ODEs (21) defines a positive dynamical system on* $\mathbb{R}^4_+$.
(b) *Under assumptions (14) and (15), the system has a positive equilibrium* $EE^{\#} = (I^*, Y^*, F^*, M^{\#}(Y_P))^T$, *where*

$$M^{\#}(Y_P) = \frac{(1-r)\nu_I(Y^* + Y_P)}{\mu_M(Y^* + Y_P) + \alpha Y_P} I^* = \frac{M^*}{1 + \frac{\alpha Y_P}{\mu_M(Y^* + Y_P)}},$$

which is globally asymptotically stable on $\mathbb{R}^4_+ \setminus \{x \in \mathbb{R}^4_+ : I = Y = F = 0\}$.

The equilibrium $EE^{\#}$ is an a regular equilibrium of (18) if and only if

$$Y^* + Y_P < \gamma M^{\#}(Y_P)$$

or, equivalently,

$$Y_P < Y_P^* := \frac{\gamma M^* - Y^*}{1 + \frac{\alpha}{\mu_M}} = \frac{1}{\mu_M + \alpha}\left(\gamma(1-r)\nu_I - \frac{r\nu_I(\delta + \mu_F)\mu_M}{(\nu_Y + \mu_F)(\delta + \mu_F) - \delta\nu_Y}\right)\left(1 - \frac{1}{\mathcal{N}_0}\right)K. \tag{22}$$

Therefore,

$$\begin{array}{ll} \text{if } Y_P < Y_P^* & \text{then } EE^{\#} \text{ is a regular equilibrium of (18);} \\ \text{if } Y_P > Y_P^* & \text{then } EE^{\#} \text{ is a virtual equilibrium of (18).} \end{array} \tag{23}$$

The threshold value Y_P^* determines the maximum level of control below which the control has essentially no effect on an established pest population. More precisely, the effect is limited to reducing the number of males, while all other compartments remain in their natural equilibrium.

3.3.2. Case 2: male scarcity

In the region of male scarcity $\gamma M \le Y + Y_P$ the dynamics of the population is governed by the system:

$$\begin{cases} \dfrac{dI}{dt} = b\left(1 - \dfrac{I}{K}\right)F - (\nu_I + \mu_I)I, \\ \dfrac{dY}{dt} = r\nu_I I - \nu_Y \dfrac{\gamma MY}{Y + Y_P} + \delta F - \mu_F Y, \\ \dfrac{dF}{dt} = \nu_Y \dfrac{\gamma MY}{Y + Y_P} - (\delta + \mu_F)F, \\ \dfrac{dM}{dt} = (1-r)\nu_I I - (\mu_M + \alpha \dfrac{Y_P}{Y + Y_P})M. \end{cases} \tag{24}$$

The following theorem exhibits the different behaviors of the model depending on the value of Y_P which can be interpreted as the effort of the mating disruption control.

Theorem 14.

(a) *The system of ODEs (24) defines a positive dynamical system on* $\mathbb{R}^4_+$.
(b) *TE is an asymptotically stable equilibrium of this system for any* $Y_P > 0$.
(c) *There exists a threshold value* Y_P^{**} *of* Y_P *such that*
  (i) *if* $Y_P > Y_P^{**}$ *the only equilibrium of the system on* $\mathbb{R}^4_+$ *is TE;*
  (ii) *if* $0 < Y_P < Y_P^{**}$ *the system has three equilibria on* $\mathbb{R}^4_+$, *TE and two positive equilibria.*

Proof. (a) and (b) are obtained via standard considerations already discussed.

(c) Setting $\frac{dI}{dt} = 0$ in (24) yields

$$F = \frac{\nu_I + \mu_I}{b\left(1 - \frac{I}{K}\right)} I.$$

Then, from $\frac{dM}{dt} = 0$, we have

$$M = \frac{(1-r)\nu_I}{\mu_M + \alpha \frac{Y_P}{Y+Y_P}} I.$$

Further, considering that $\frac{dY}{dt} + \frac{dF}{dt} = 0$, we deduce

$$Y = \frac{r\nu_I I - \mu_F F}{\mu_F} = \left(\frac{r\nu_I}{\mu_F} - \frac{\mu_F(\nu_I + \mu_I)}{\mu_F b\left(1 - \frac{I}{K}\right)}\right) I = \frac{\phi(I)}{\mu_F b\left(1 - \frac{I}{K}\right)} I.$$

with $\phi(I) = r\nu_I b(1 - \frac{I}{K}) - \mu_F(\nu_I + \mu_I)$. Substituting the expressions of Y, F and M into the equation for $\frac{dF}{dt} = 0$, we obtain an equation for I in the form

$$\psi(I) := I\xi(I)\phi(I) = \eta(Y_P, I), \tag{25}$$

where

$$\xi(I) = \nu_Y \gamma (1-r)\nu_I b\left(1 - \frac{I}{K}\right) - (\delta + \mu_F)(\nu_I + \mu_I)\mu_M, \tag{26}$$

$$\eta(Y_P, I) = \mu_F(\delta + \mu_F)(\nu_I + \mu_I)(\mu_M + \alpha) b\left(1 - \frac{I}{K}\right) Y_P. \tag{27}$$

Therefore, the non-trivial equilibria of (24) are of the form

$$Y_{MD} = \left(\frac{r\nu_I}{\mu_F} - \frac{\mu_F(\nu_I + \mu_I)}{\mu_F b\left(1 - \frac{I_{MD}}{K}\right)}\right) I_{MD}, \tag{28}$$

$$F_{MD} = \frac{\nu_I + \mu_I}{b\left(1 - \frac{I_{MD}}{K}\right)} I_{MD}, \tag{29}$$

$$M_{MD} = \frac{(1-r)\nu_I}{\mu_M + \alpha \frac{Y_P}{Y_{MD}+Y_P}} I_{MD}. \tag{30}$$

with I_{MD} a positive root of (25). Further, we note that to ensure $Y_{MD} > 0$, it follows from (28) that I_{MD} must satisfy the condition

$$I_{MD} < K\left(1 - \frac{\mu_F(\nu_I + \mu_I)}{r\nu_I b}\right). \tag{31}$$

Thus, to obtain biologically viable equilibria, I_{MD} must belong to the interval $[0, K(1 - \frac{\mu_F(\nu_I+\mu_I)}{r\nu_I b})]$.

The roots of (25) correspond to the values of I where the graph of the cubic polynomial ψ and the straight line $\eta(Y_P,\cdot)$ intersect. It is clear that, the straight line $\eta(Y_P,\cdot)$ intersects the I-axis at $I = K$. From the factorization of $\psi(I)$ in (25), it is clear that the roots of ψ are

$$I_0 = 0, \quad I_1 = K\left(1 - \frac{(\delta + \mu_F)(\nu_I + \mu_I)\mu_M}{\nu_Y \gamma (1-r)\nu_I b}\right), \text{ and } I_2 = K\left(1 - \frac{\mu_F(\nu_I + \mu_I)}{r\nu_I b}\right). \tag{32}$$

Note that the the roots I_1 and I_2, are positive and smaller than K, i.e. $0 < I_1, I_2 < K$, provided

$$\frac{(\delta + \mu_F)(\nu_I + \mu_I)\mu_M}{\nu_Y \gamma (1-r)\nu_I b} < 1, \tag{33}$$

and respectively,

$$\frac{\mu_F(\nu_I + \mu_I)}{r\nu_I b} < 1. \tag{34}$$

Inequality (33) is satisfied under assumptions (15) and (14), and inequality (34) is equivalent to $\mathcal{N}_0 > 1$, that is, to (14). Therefore, under assumptions (14) and (15), we have that $I_1, I_2 \in [0, K]$. Therefore, the graph of the cubic polynomial ψ is as given on Fig. 3.

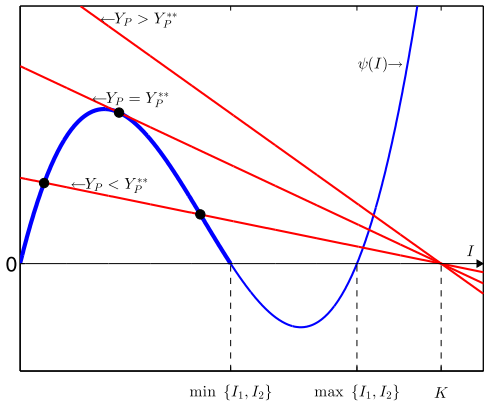

Fig. 3. Intersections between the graphs of $\eta(Y_P,\cdot)$ (in red) and ψ (in blue) for different values of Y_P. The black dots represent the intersection points on the interval $[0, \min\{I_1, I_2\}]$. (For interpretation of the references to color in this figure legend, the reader is referred to the web version of this article.)

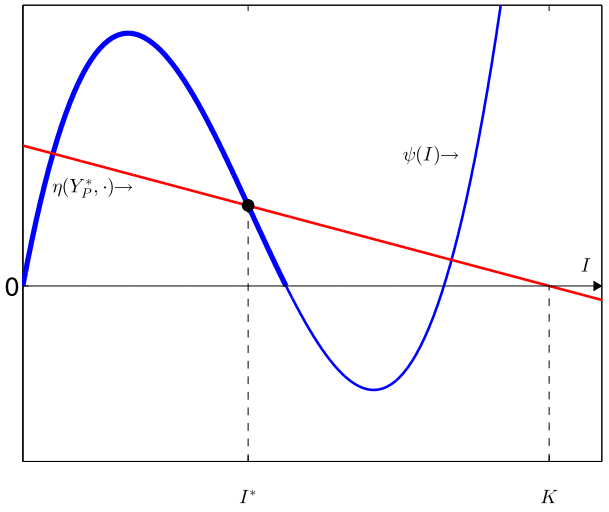

Fig. 4. Intersections between the graphs of $\eta(Y_P^*,\cdot)$ (in red) and ψ (in blue). The black dot represent the intersection for $I = I^*$. (For interpretation of the references to color in this figure legend, the reader is referred to the web version of this article.)

Considering the inequality (31), only points of intersection of the straight line $\eta(Y_P,\cdot)$ with the section of the graph of ψ for $0 \le I \le \min\{I_1, I_2\}$, indicated by a thicker line on Fig. 3, are of relevance to the equilibria of the model. Let us note that ψ is independent of Y_P while the gradient of the line η is a multiple of Y_P. We denote by Y_P^{**} the value of Y_P such that the line $\eta(Y_P,\cdot)$ is tangent to the indicated section of the graph of ψ, see Fig. 3. Then it is clear that for $Y_P > Y_P^{**}$ there is no intersection between $\eta(Y_P,\cdot)$ and ψ on $[0, \min\{I_1, I_2\}]$ while if $0 < Y_P < Y_P^{**}$ there are two such points of intersection. This proves items (i) and (ii) in (c). □

3.4. Conclusions for the model (18)

Let $I_{MD}^{(1)}$ and $I_{MD}^{(2)}$, $I_{MD}^{(1)} < I_{MD}^{(2)}$, be the roots of (25) when $0 < Y_P < Y_P^{**}$ and denote the respective equilibria by $EE_{MD}^{(1)}$ and $EE_{MD}^{(2)}$.

We saw already in (23) that $EE^{\#}$ is a regular or virtual equilibrium according as $Y_P < Y_P^*$ or $Y_P > Y_P^*$. For $Y = Y_P^*$ we have $EE^{\#} \in \Sigma(Y_P)$, that is $EE^{\#}$ is a boundary equilibrium. Due to the continuity of $g(x, Y_P)$, $EE^{\#}$ is an equilibrium of (24). Hence, $EE^{\#} = EE_{MD}^{(2)}$ for $Y_P = Y_P^*$.

One can see from Fig. 4 that for $0 < Y_P < Y_P^*$, we have

$$I_{MD}^{(1)} < I^* < I_{MD}^{(2)}, \tag{35}$$

while for $Y_P^* < Y_P < Y_P^{**}$, we have

$$I_{MD}^{(1)} < I_{MD}^{(2)} < I^*. \tag{36}$$

We investigate when the equilibria of (24) are regular equilibria of (18), that is when they belong to the male scarcity region. After some technical manipulations we have

$$\begin{aligned} &Y_{MD}+Y_P-\gamma M_{MD}\\ &=\left(\frac{\mu_M}{\mu_M+\alpha\frac{Y_P}{Y_{MD}+Y_P}}\left(\frac{r\nu_I}{\mu_F}-\frac{\mu_F(\nu_I+\mu_I)}{\mu_F\left(1-\frac{I_{MD}}{K}\right)}\right)-\gamma(1-r)\nu_I\right)I_{MD}+(\mu_M+\alpha)Y_P. \end{aligned}$$

Let $Y_P^* < Y_P < Y_P^{**}$. Then using also (36) we have

$$\begin{aligned} &Y_{MD}+Y_P-\gamma M_{MD}\\ &\geq\left(\frac{\mu_M}{\mu_M+\alpha\frac{Y_P}{Y_{MD}+Y_P}}\left(\frac{r\nu_I}{\mu_F}-\frac{\mu_F(\nu_I+\mu_I)}{\mu_F\left(1-\frac{I^*}{K}\right)}\right)-\gamma(1-r)\nu_I\right)I_{MD}+(\mu_M+\alpha)Y_P \qquad (37)\\ &=\left(\left(\mu_M\frac{r\nu_I(\delta+\mu_F)}{\nu_Y\mu_F+\mu_F\mu_F+\delta\mu_F}\right)-\gamma(1-r)\nu_I\right)I_{MD}+(\mu_M+\alpha)Y_P \quad \text{(using (22))}\\ &=-(\mu_M+\alpha)\frac{Y_P^*}{I^*}I_{MD}+(\mu_M+\alpha)Y_P\\ &=\frac{\mu_M+\alpha}{I^*}(Y_PI^*-Y_P^*I_{MD})>0. \end{aligned}$$

Therefore, in this case $EE_{MD}^{(1)}$ and $EE_{MD}^{(2)}$ are both in the male scarcity region. Hence, they are regular equilibria of (18).

If $Y_P < Y_P^*$ and $I_{MD} > I^*$, considering (35) and using the same method as in (37) we obtain

$$Y_P+Y_{MD}-\gamma M_{MD}<0. \qquad (38)$$

Therefore, $EE_{MD}^{(2)}$ is not in the male scarcity region. Hence, it is a virtual equilibrium of (18).

Taking into consideration the above results regarding $EE^{\#}$, $EE_{MD}^{(1)}$ and $EE_{MD}^{(2)}$ we obtain the following theorem for the model (18).

Theorem 15. *Let $Y_P > 0$. The following holds for model (18):*

(a) *TE is an asymptotically stable equilibrium.*
(b) *If $0 < Y_P < Y_P^*$ there are two positive equilibria $EE_{MD}^{(1)}$ and $EE^{\#}$, where $EE^{\#}$ is asymptotically stable.*
(c) *If $Y_P^* < Y_P < Y_P^{**}$ there are two positive equilibria $EE_{MD}^{(1)}$ and $EE_{MD}^{(2)}$.*
(d) *If $Y_P > Y_P^{**}$ there is no positive equilibrium.*

Remarks. 1. In the theory of PWS systems, the bifurcation at $Y_P = Y_P^*$ is called a discontinuity induced border crossing bifurcation. As Y_P increases and passes through Y_P^* the regular equilibrium $EE^{\#}$ collides with the virtual equilibrium $EE_{MD}^{(2)}$ on the boundary $\Sigma(Y_P)$ and they exchange properties, that is $EE^{\#}$ becomes virtual while $EE_{MD}^{(2)}$ becomes regular.

2. The bifurcation at $Y_P = Y_P^{**}$ is not discontinuity induced since for $Y_P = Y_P^{**}$ the two regular equilibria $EE_{MD}^{(1)}$ and $EE_{MD}^{(2)}$ are both in the interior of the male scarcity region. We have a saddle point bifurcation: as Y_P increases through Y_P^{**} the equilibria $EE_{MD}^{(1)}$ and $EE_{MD}^{(2)}$ collide and disappear.

Obtaining theoretically the stability properties of the equilibria $EE_{MD}^{(1)}$ and $EE_{MD}^{(2)}$ is not easy considering the complexity of the system. The numerical simulations indicate that $EE_{MD}^{(1)}$ is unstable while $EE_{MD}^{(2)}$ is asymptotically stable, and that the equilibria are the only invariant set of the system on $\mathbb{R}_4^+$. Further, when $Y_P > Y_P^{**}$, *TE* is globally asymptotically stable. The equilibria and their properties are presented on the bifurcation diagram in Fig. 5. The equilibrium values of $Y + F$ are given as function of the bifurcation parameter Y_P. The solid line represents stable equilibria, while the dotted line represents unstable equilibria.

3.4.1. Global asymptotic stability of the trivial equilibrium for sufficiently large Y_P

Theorem 15 shows that for $Y_P < Y_P^{**}$ the insect population persists at substantial endemic level. More precisely, and as illustrated in Fig. 5, the control has practically no effect ($Y_P < Y_P^*$) or provides only for minor reduction ($Y_P^* < Y_P < Y_P^{**}$) of an established population, e.g. at its natural equilibrium. Hence, the numerically observed global asymptotic stability of *TE*, that is, eventual population extinction, for $Y_P > Y_P^{**}$ is of significant practical importance. This section deals with the mathematical proof of this result. More precisely, we will establish global asymptotic stability of *TE* under slightly stronger condition $Y_P > \tilde{Y}_P^{**}$ where $\tilde{Y}_P^{**} > Y_P^{**}$. We also show that $\tilde{Y}_P^{**}$ is a close approximation for Y_P^{**}. The asymptotic analysis for system (18) cannot be conducted in the same way as for the other systems considered so far, since it is not a collaborative system. More precisely due to the term $-\nu_Y\frac{\gamma M}{Y+Y_P}Y$ in the equation for the Y compartment, the right hand side of (18) is not quasi-monotone. In order to obtain the practically important result mentioned above, we consider an auxiliary system which

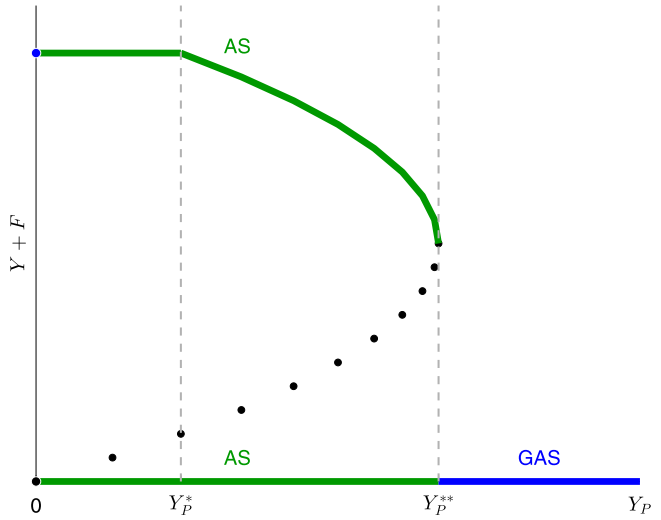

Fig. 5. Bifurcation diagram of the values of $Y+F$ at equilibrium with respect to the values of Y_P for system (18).

is collaborative and provides upper bounds for the solutions of (18). The system is obtained by removing the mentioned term in the second equation and replacing $\min\{\frac{\gamma M}{Y+Y_P}, 1\}$ by $\frac{\gamma M}{Y+Y_P}$ in the third equation. In vector form it is given as

$$\frac{dx}{dt} = \tilde{h}(x), \tag{39}$$

where $x = (I, Y, F, M)^T$ and

$$\tilde{h}(x) = \begin{pmatrix} b\left(1-\frac{I}{K}\right)F - (\nu_I + \mu_I)I \\ r\nu_I I - \mu_F Y + \delta F \\ \nu_Y \frac{\gamma M}{Y+Y_P} Y - \delta F - \mu_F F \\ (1-r)\nu_I I - (\mu_M + \alpha \frac{Y_P}{Y+Y_P})M \end{pmatrix}. \tag{40}$$

It is easy to see that function $\tilde{h}$ is quasi-monotone on $\Omega_K = \{x \in \mathbb{R}^4_+ : I \le K\}$.

Theorem 16.

(a) *The system of ODEs (39) defines a positive dynamical system on* $\mathbb{R}^4_+$.
(b) *TE is asymptotically stable equilibrium.*
(c) *There exists a threshold value* $\tilde{Y}_P^{**}$ *such that*
  (i) *if* $Y_P > \tilde{Y}_P^{**}$, *TE is globally asymptotically stable on* $\mathbb{R}^4_+$;
  (ii) *if* $0 < Y_P < \tilde{Y}_P^{**}$, *the system has three equilibria, TE and two positive equilibria* $\tilde{E}^{(1)}$ *and* $\tilde{E}^{(2)}$ *such that* $\tilde{E}^{(1)} < \tilde{E}^{(2)}$. *The basin of attraction of TE contains the set* $\{x \in \mathbb{R}^4_+ : 0 \le x < \tilde{E}^{(1)}\}$. *The basin of attraction of* $\tilde{E}^{(2)}$ *contains the set* $\{x \in \mathbb{R}^4_+ : x \ge \tilde{E}^{(2)}, I \le K\}$.

Proof. (a) and (b) are proved similarly to Theorem 14 are obtained via standard techniques.
(c) Setting the first, second and fourth component of $\tilde{h}$ to zero, we have

$$Y = \frac{r\nu_I I + \delta F}{\mu_F}, \quad F = \frac{\nu_I + \mu_I}{b\left(1-\frac{I}{K}\right)} I, \quad M = \frac{(1-r)\nu_I}{\mu_M Y + (\mu_M + \alpha)Y_P} I.$$

Setting the third component of $\tilde{h}$ to zero and substituting the expressions for Y, F and M above and following the method in the proof of point (c) in Theorem 14, we obtain an equation for I which is similar to (25) but with a different cubic. More precisely, the equation for I is in the form

$$\tilde{\psi}(I) := I\xi(I)\tilde{\phi}(I) = \eta(Y_P, I), \tag{41}$$

where $\xi(I)$ and $\eta(Y_P, I)$ are the linear expression given in (26) and (27) and

$$\tilde{\phi}(I) = r\nu_I b\left(1 - \frac{I}{K}\right) + \delta(\nu_I + \mu_I). \tag{42}$$

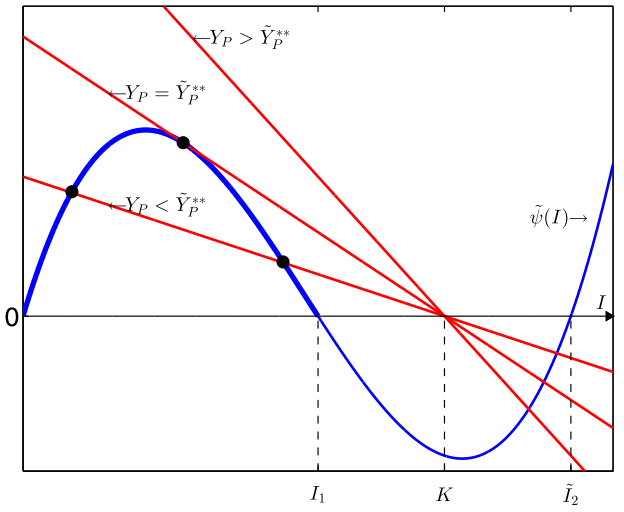

Fig. 6. Intersections between the graphs of $\eta(Y_P,\cdot)$ (in red) and ψ (in blue) for different values of Y_P. The black dots represent the intersection points on the interval $[0, I_1]$. (For interpretation of the references to color in this figure legend, the reader is referred to the web version of this article.)

Therefore the non-trivial equilibria of (39) are of the form

$$\begin{aligned}\tilde{Y} &= \frac{1}{\mu_F}\left(r\nu_I + \frac{\delta(\nu_I+\mu_I)}{b\left(1-\frac{\tilde{I}}{K}\right)}\right)\tilde{I},\\ \tilde{F} &= \frac{\nu_I+\mu_I}{b\left(1-\frac{\tilde{I}}{K}\right)}\tilde{I},\\ \tilde{M} &= \frac{(1-r)\nu_I}{\mu_M+\alpha\frac{Y_P}{\tilde{Y}+Y_P}}\tilde{I},\end{aligned} \tag{43}$$

with $\tilde{I}$ a positive root of (41). The roots of (41) correspond to the values of I where the graph of the cubic polynomial $\tilde{\psi}$ and the straight line $\eta(Y_P,\cdot)$ intersect. It is clear that the straight line $\eta(Y_P,\cdot)$ intersects the I axis at $I = K$. Note that the state where I greater is than K is not sustainable, and therefore not biologically relevant. From the factorization of $\tilde{\psi}$ in (41), it is clear that I_0 and I_1 given in (32) and

$$\tilde{I}_2 = \left(1+\frac{\delta(\nu_I+\mu_I)}{r\nu_I b}\right)K \tag{44}$$

are roots of $\tilde{\psi}$. Clearly, we have

$$0 < I_1 < K < \tilde{I}_2. \tag{45}$$

Therefore, the graph of the cubic polynomial $\tilde{\psi}$ is as given in Fig. 6.

Considering the inequality (45), only the points of intersection of the straight line $\eta(Y_P,\cdot)$ with the section of the graph of $\tilde{\psi}$ for $0 < I < I_1$ are of relevance to the equilibria of the model. Note that $\tilde{\psi}$ is independent of Y_P while the gradient of $\eta(Y_P,\cdot)$ is a multiple of Y_P. We denote by $\tilde{Y}_P^{**}$ the value of Y_P such that the line η is tangent to the indicated section of the graph of $\tilde{\psi}$, see Fig. 6. Then, it is clear that for $Y_P > \tilde{Y}_P^{**}$ there is no intersection between $\eta(Y_P,\cdot)$ and $\tilde{\psi}$ on $[0, I_1]$ while if $0 < Y_P < \tilde{Y}_P^{**}$ there are two such points of intersection.

(i) Let $Y_P > \tilde{Y}_P^{**}$. Consider the point

$$\tilde{y}_q = \begin{pmatrix} K \\ \frac{1}{\mu_F}\left(r\nu_I + \frac{\delta\nu_Y\gamma(1-r)\nu_I}{(\delta+\mu_F)\mu_M}\right)q \\ \frac{\nu_Y\gamma(1-r)\nu_I}{(\delta+\mu_F)\mu_M}q \\ \frac{(1-r)\nu_I}{\mu_M}q \end{pmatrix}, \tag{46}$$

where $q \in \mathbb{R}, q \geq K$. It is easy to see that $\tilde{h}(\tilde{y}_q) \leq 0$. Then by Theorem 7, *TE* is GAS on $[\mathbf{0}, \tilde{y}_q]$. Therefore, *TE* is GAS on $\cup_{q\geq K}[\mathbf{0}, \tilde{y}_q] = \Omega_K$ as well. Similarly to Theorem 9, Ω_K is an absorbing set. Hence *TE* is GAS on $\mathbb{R}^4_+$.

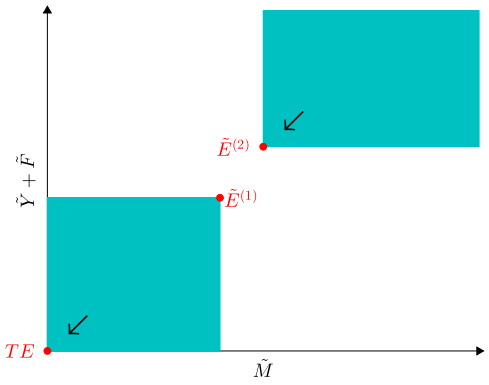

Fig. 7. Positive invariant sets, when $0 < Y_P < \tilde{Y}_P^{**}$.

(ii) Let $0 < Y_P < \tilde{Y}_P^{**}$. Denote the two equilibria by $\tilde{E}^{(j)} = (\tilde{I}^{(j)}, \tilde{Y}^{(j)}, \tilde{F}^{(j)}, \tilde{M}^{(j)})^T$, $j = 1, 2$, where $\tilde{I}^{(1)} < \tilde{I}^{(2)}$. Since $\tilde{Y}$, $\tilde{F}$, $\tilde{M}$ as given in (43) are increasing functions of $\tilde{I}$, we have $0 < \tilde{E}^{(1)} < \tilde{E}^{(2)}$ (Fig. 7). Using that $\tilde{h}(\tilde{y}_q) \leq 0 = \tilde{h}(\tilde{E}^{(2)})$, by Theorem 7 $\tilde{E}^{(2)}$ is GAS on $[\tilde{E}^{(2)}, \tilde{y}_q]$. Therefore, $\tilde{E}^{(2)}$ is GAS on $\cup_{q\geq K}[\tilde{E}^{(2)}, \tilde{y}_q] = \{x \in \mathbb{R}^4_+ : x \geq \tilde{E}^{(2)}, I \leq K\}$. We obtain the statements about the basin of attraction of *TE* by using Theorem 8. Indeed, *TE*, being asymptotically stable, attracts some solutions initiated in $[TE, \tilde{E}^{(1)}]$. Then it follows from Theorem 8 that all solutions initiated in $\{x \in \mathbb{R}^4_+ : x < \tilde{E}^{(1)}\}$ converge to *TE*. □

Let us recall that we consider the system (39) as an approximation to (18) with the aim of providing conditions for insect pest extinction – the most desirable outcome of a control strategy. A four dimensional dynamical systems like (18) may, in general, have invariant sets of different nature. The result in Theorem 15 that for $Y > Y_P^{**}$ *TE* is the only equilibrium of (18) and that it is asymptotically stable, does not exclude the possibility of existence of other invariant sets of the system in $\mathbb{R}^4_+$. Using Theorem 16 for the auxiliary system (18) we prove the following theorem which provides statements for the basin of attraction of *TE* and particularly includes a sufficient condition for pest population extinction, that is TE being GAS.

Theorem 17. *Let $Y_P > 0$. Then the following hold for the model (18).*

(a) *If $0 < Y_P \leq \tilde{Y}_P^{**}$, then the basin of attraction of TE contains $\{x \in \mathbb{R}^4_+ : x < \tilde{E}^{(1)}\}$.*
(b) *If $Y_P > \tilde{Y}_P^{**}$, then TE is GAS on $\mathbb{R}^4_+$.*

Proof. Using the monotonicity theorem [22, 8.XI] with x being the solution of (39) and y being the solution of (18) we obtain that any solution of (39) is an upper bound of the solution of (18) with the same initial point. This implies that the basin of attraction of *TE* as an equilibrium of (18) contains the sets indicated in Theorem 16 (c) (i) and (ii), thus proving (a) and (b), respectively. □

Theorem 17 characterizes the benefit from the control effort represented by Y_P as follows:

- Increasing the effort Y_P in the range $0 < Y_P < Y_P^{**}$ does not lead to elimination of an established population. In fact, as shown on Fig. 5, the reduction is not proportional to the effort. However, $\tilde{E}^{(1)}$ increases at least linearly with $\tilde{I}^{(1)}$. Hence, increasing Y_P enlarges the basin of attraction of *TE*, providing better opportunity for controlling an invading population.
- Effort Y_P stronger than $\tilde{Y}_P^{**}$ eliminates any established or invading population.

4. Numerical simulation and discussion

We use numerical simulations to illustrate the results of Theorems 15 and 17 and discuss the biological meaning of the results. The numerical simulations are done using the **ode23tb** solver of Matlab [23] which solves system of stiff ODEs using a trapezoidal rule and second order backward differentiation scheme (TR-BDF2) [24,25]. The values of the parameters used for the numerical simulations are those of Table 1.

Using (9), we compute the basic offspring number, $\mathcal{N}_0 = 122$. $\mathcal{N}_0 > 1$, therefore, the population establishes to the positive endemic equilibrium EE^* which we have shown to be GAS on $\mathbb{R}^4_+ \setminus \{TE\}$ (Theorem 9 (c)). Fig. 8 represents the trajectories of a set of solutions of system (1), or equivalently system (18) with $Y_P = 0$ and $\alpha = 0$, in the $M \times (Y + F)$ plane. The dots represent the points at which the solutions are initiated. The solutions initiated on $\mathbb{R}^4_+ \setminus \{TE\}$ all converge to the point $EE^* = (992, 319, 1407, 1498)^T$, represented by the green square. Here, *TE* is also an equilibrium, but it is unstable (Theorem 9 (c)), and therefore it is not represented in Fig. 8.

In the following, we confirm numerically the theoretical results of Theorems 15 and 17 with respect to the values of the mating disruption thresholds mentioned in those theorems, Y_P^* and Y_P^{**}. We also investigate the impact of the trapping effort,

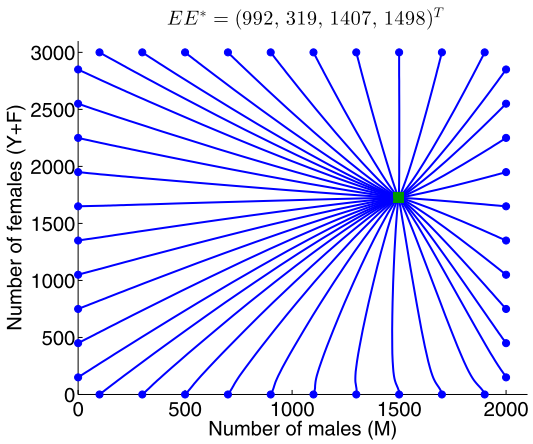

Fig. 8. Trajectories of a set solutions of system (1) in the $M \times (Y + F)$-plane initiated at the dots. The green square represents the stable equilibrium EE^*. (For interpretation of the references to color in this figure legend, the reader is referred to the web version of this article.)

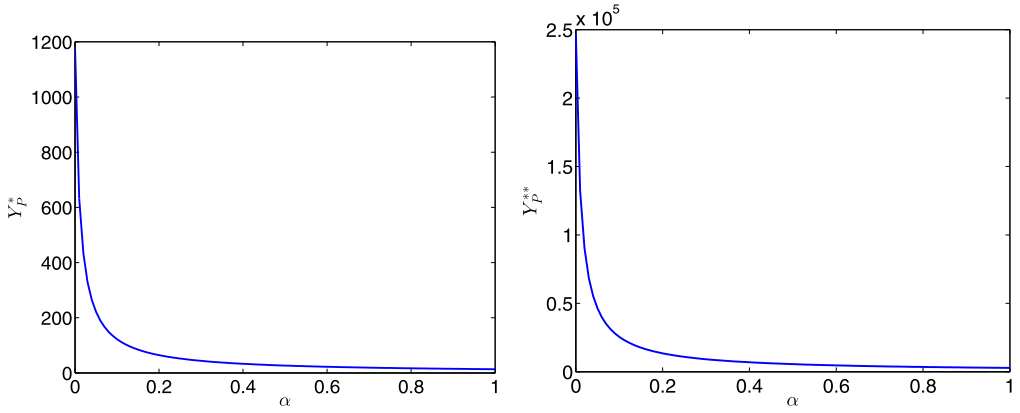

(a) Y_P^* as a function of α (b) Y_P^{**} as a function of α

Fig. 9. Mating disruption thresholds as function of the trapping parameter α.

α, on the population. Using (22) and solving numerically the system

$$\begin{cases} \psi(I) = \eta(Y_P, I) \\ \dfrac{d\psi}{dI}(I) = \dfrac{d\eta}{dI}(Y_P, I) \end{cases}$$

with ψ and $\eta(Y_P,\cdot)$ as defined in (25), we obtain respectively the thresholds values Y_P^* and Y_P^{**} as functions of α as represented in Fig. 9.

One can observe that a small trapping effort reduces the mating disruption thresholds in a non-linear manner. Adding trapping to mating disruption allows to reduce the amount of the lure for equivalent control efficiency. In particular, for $\alpha = 0$, we have $Y_P^* = 5673$ and $Y_P^{**} = 987,735$, while for $\alpha = 0.1$, we have $Y_P^* = 588$ and $Y_P^{**} = 102,462$. Thus, increasing the trapping effort by 10% reduces both Y_P^* and Y_P^{**} by 90%.

Fig. 10 illustrates the trajectories of the solutions of system (18) when the mating disruption level is below the threshold Y_P^* for $\alpha = 0$ and $\alpha = 0.1$. The dots represent the initial points and the green squares represent the asymptotically stable equilibria. In this case, the system has one positive equilibrium, $EE^{\#}$ (Theorem 15 (b)), with value given in the figure. One can observe that when there is no trapping, $EE^{\#} = EE^*$ (Fig. 10(a)). This means that the positive endemic equilibrium of the population is not affected by the control. When trapping occurs, we observe in Fig. 10(b) that the positive equilibrium is shifted to the left. In fact, the control allows to reduce the number of males but not sufficiently to disrupt the fertilization of the females. Therefore, the control is not efficient on an established population as the number of females at equilibrium is not reduced.

However, when $Y_P > 0$, TE is asymptotically stable, which means that a population can be controlled if it is small enough. Fig. 11(a), represents the basin of attraction of TE (the red dots) for a small population in the same setting as for the experiments in Fig. 10(a). We observe that there is a set of solutions, for which the initial population is small enough, that converge

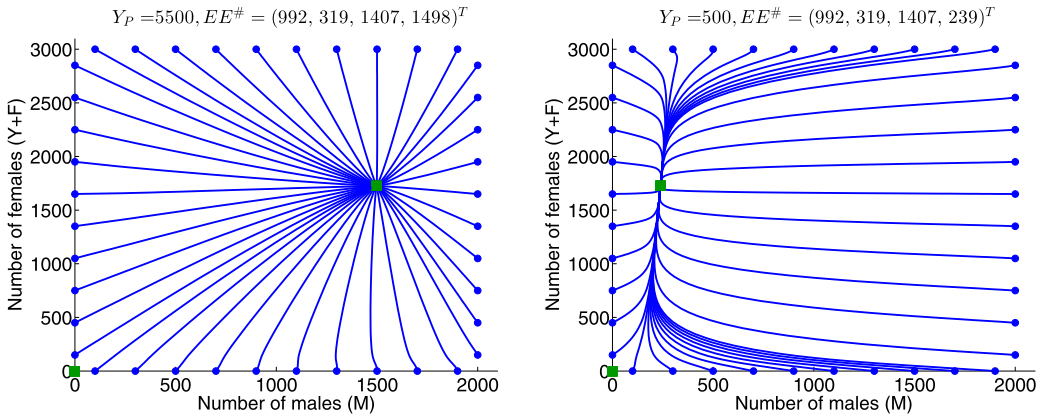

(a) $\alpha = 0$ (b) $\alpha = 0.1$

Fig. 10. Trajectories of a set solutions of system (18) in the $M \times (Y + F)$-plane initiated at the dots. The green squares represent the asymptotically stable equilibria *TE* and $EE^{\#}$. (For interpretation of the references to color in this figure legend, the reader is referred to the web version of this article.)

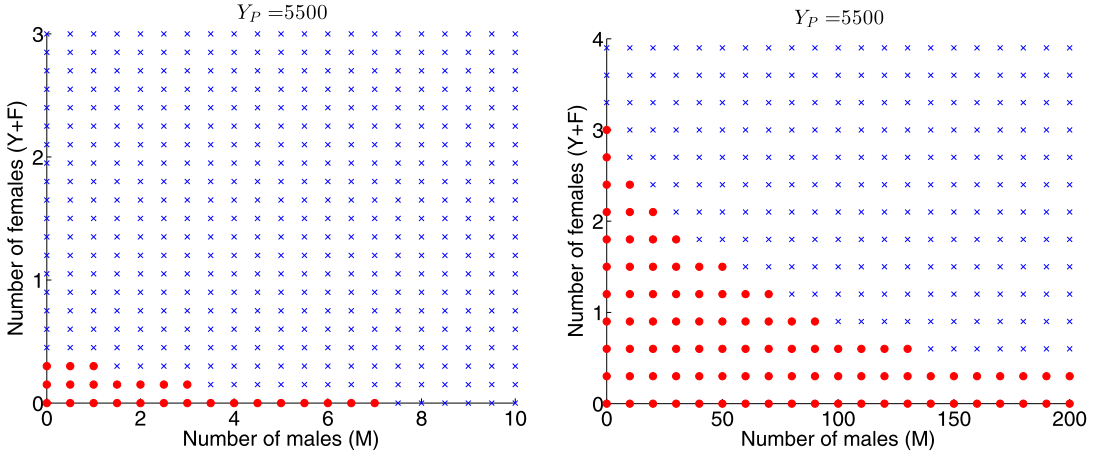

(a) $\alpha = 0.$ (b) $\alpha = 0.1.$

Fig. 11. Effect of α on the basin of attraction of *TE*. The solutions initiated at the points represented by the red dots converge to *TE* while the blue crosses represent initial points for which the solution converges to $EE^{\#}$. (For interpretation of the references to color in this figure legend, the reader is referred to the web version of this article.)

to *TE*, hence, a small population can be eradicated for $Y_P > 0$. Further, as shown in Fig. 11(b), adding trapping ($\alpha = 0.1$) with the same mating disruption effort as for Fig. 11(a), enlarges the basin of attraction of *TE*. In other words, for identical mating disruption effort, larger populations can be drawn to extinction when trapping occurs.

In order to observe a reduction in the number of females, the mating disruption effort has to be increased above the threshold Y_P^*. This is the case in Fig. 12((a) and (b)), where $Y_P = 0.9999 \times Y_P^{**} < Y_P^*$, for $\alpha = 0$ and $\alpha = 0.1$, respectively. We can see that there is a positive asymptotically stable equilibrium, $EE_{MD}^{(2)}$ represented with a green square (Theorem 15 (c)). The blue lines represent the trajectories of the solutions of (18) initiated at the blue points which converge to $EE_{MD}^{(2)}$, while the red lines represent the trajectories of the solutions initiated at the red points which converge to *TE*. With $Y_P > Y_P^*$, the number of females at equilibrium is reduced, however, the impact of the control is not proportional to the effort. Indeed comparing the experiments in Figs. 10 and12, we observe that in order to reduce the number of females at equilibrium by 49%, the amount of the lure has to be increased by 17, 857% when $\alpha = 0$ and by 20, 390% when $\alpha = 0.1$.

Further, comparing the red dots in Fig. 11 and the red trajectories in Fig. 12, we can see that the basin of attraction of the trivial equilibrium becomes larger as the value of Y_P increases.

Finally, $Y_P > Y_P^{**}$ allows a full control of the population leading it to extinction no matter how big it is. In Fig. 13, Y_P is above Y_P^{**} by 0.01%, and we can see that all the trajectories converge to *TE*. This shows the GAS nature of *TE* when $Y_P > Y_P^{**}$.

Note that in Theorem 17, the GAS of *TE* is established for $Y_P > \tilde{Y}_P^{**}$, however, we show numerically that the GAS property of *TE* holds for $Y_P > Y_P^{**}$. From Fig. 14 we can see that the error between $\tilde{Y}_P^{**}$ and Y_P^{**} is of order 10^4 which is small compared to the values of $\tilde{Y}_P^{**}$ and Y_P^{**} which are of order 10^6.

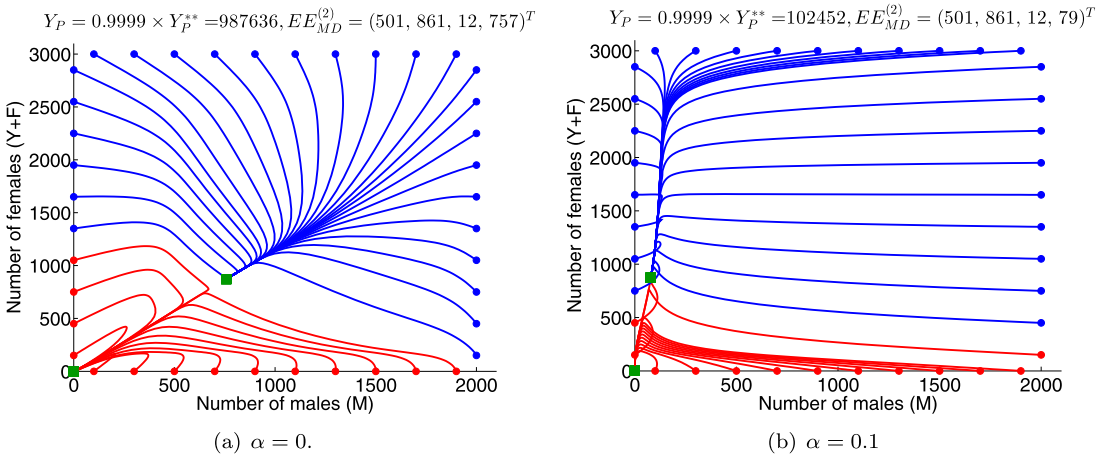

(a) $\alpha = 0.$ (b) $\alpha = 0.1$

Fig. 12. Trajectories of a set solutions of system (18) in the $M \times (Y + F)$-plane initiated at the dots. The green squares represent the asymptotically stable equilibria. (For interpretation of the references to color in this figure legend, the reader is referred to the web version of this article.)

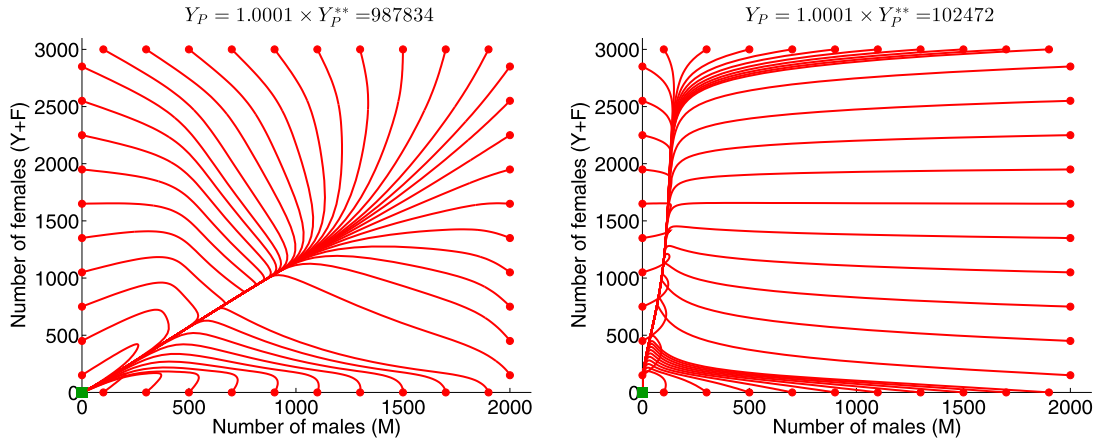

(a) $\alpha = 0.$ (b) $\alpha = 0.1$

Fig. 13. Trajectories of a set solutions of system (18) in the $M \times (Y + F)$-plane initiated at the dots. The green squares represent the asymptotically stable equilibria. (For interpretation of the references to color in this figure legend, the reader is referred to the web version of this article.)

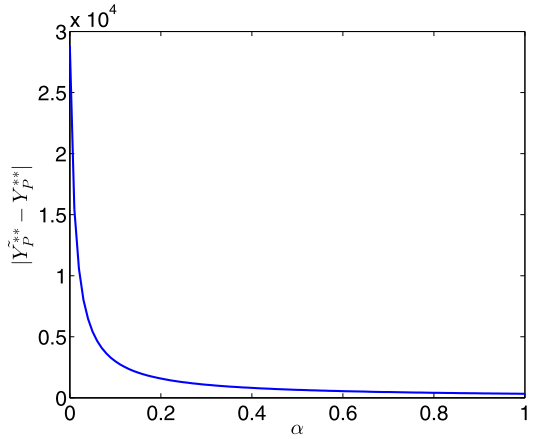

Fig. 14. Error between the thresholds $\tilde{Y}_P^{**}$ and Y_P^{**} as function of α.

5. Conclusion and perspectives

Controlling insect pest population in environmentally respectful manner is a main challenge in IPM programs. Mating disruption using female sex-pheromone based lures falls within IPM requirements as it is species specific and leaves no toxic residues in the produce grown. In this work, we build a generic model, governed by a system of piecewise-smooth continuous ODEs to simulate the dynamics of a pest population and its response to mating disruption control with trapping. From the theoretical analysis of the model, we identify two threshold values of biological interest for the strength of the lure. The first threshold, Y_p^*, corresponds to a minimum amount of pheromone necessary for mating disruption to have an effect on the population. However, we show that the control can only be fully efficient, that is, drive an established population to extinction, for an amount of pheromone above a second threshold, Y_p^{**}. We also show asymptotic stability of the trivial equilibrium, *TE*, whenever $Y_P > 0$. In other words, a small amount of pheromone can be efficient on a very small population, like at invasion stage. These theoretical results are consistent with field observation, where the failure of mating disruption is often attributed to a wrong dosage of the pheromone and/or to an excessive population density [10,11].

Further, we show that increasing the capture efficiency of the traps can reduce considerably these threshold values. From practical point of view this suggests that there is an optimal combination of the strength of the pheromone attractant and the capture efficiency of the traps to optimize the control of the pests in terms of population control and cost. These results support the conclusions of Yamanaka [26] stipulating that in the case where the lure used for mating disruption is strong enough, then additional trapping is not necessary, while otherwise, the author advise to rather focus the effort on the trapping efficiency. In a more realistic setting, this optimized control corresponds to an optimal setting of traps releasing the pheromone. Alternative approaches, such as individual based models, have been considered to study the impact of mating disruption, incorporating a spatial component where the attraction of males is governed by the pheromone plume [27], or by the effective attraction radius which corresponds to the probability of finding the source [28]. A next step for this work is to add a spatial component to investigate how traps should be set, how many should be used, and how far from each other they should be positioned. Investigation on trap settings and their interactions have been studied in a parallel work dealing with parameter estimation [29] and extended in [30], where spatio-temporal trapping models are governed by advection–diffusion–reaction processes. Finally, field experiments would be welcome to validate the threshold parameters and the model.

Acknowledgments

This work has been supported by the French Ministry of Foreign Affairs and International Development and the South African National Research Foundation in the framework of the PHC PROTEA 2015 call, PHC no 38879RD. The support of the DST/NRF Centre of Excellence in Mathematical and Statistical Sciences (CoE-MaSS) and the DST/NRF SARChI Chair in Mathematical Methods and Models in Biosciences and Bioengineering towards this research is hereby acknowledged. Opinions expressed and conclusions arrived at, are those of the authors and are not necessarily to be attributed to the CoE or the SARChI Chair.

The authors thank the anonymous reviewers and the handling editor for fruitful comments that greatly improve the initial manuscript.

References

[1] J.L. Apple, R.F.E. Smith, Integrated Pest Management, Plenum Press, New-York, 1976.
[2] P. Witzgall, P. Kirsch, A. Cork, Sex pheromones and their impact on pest management, J. Chem. Ecol. 36 (1) (2010) 80–100.
[3] P.E. Howse, I.D. Stevens, O.T. Jones, Insect Pheromones and Their Use in Pest Management, Chapman & Hall, 1998.
[4] R. Bartell, Mechanisms of communication disruption by pheromone in the control of lepidoptera: a review, Physiol. Entomol. 7 (4) (1982) 353–364.
[5] R.T. Carde, Principles of mating disruption, Behavior-Modifying Chemicals for Pest Management: Applications of Pheromones and Other Attractants, Marcel Dekker, New York, 1990, pp. 47–71.
[6] A. Cocco, S. Deliperi, G. Delrio, Control of *Tuta absoluta* (Meyrick) (Lepidoptera: Gelechiidae) in greenhouse tomato crops using the mating disruption technique, J. Appl. Entomol. 137 (1–2) (2013) 16–28.
[7] R.T. Carde, A.K. Minks, Control of moth pests by mating disruption: successes and constraints, Ann. Rev. Entomol. 40 (1) (1995) 559–585.
[8] S. Vacas, C. Alfaro, J. Primo, V. Navarro-Llopis, Deployment of mating disruption dispensers before and after first seasonal male flights for the control of aonidiella aurantii in citrus, J. Pest Sci. 88 (2) (2015) 321–329.
[9] L.L. Stelinski, J.R. Miller, M.E. Rogers, Mating disruption of citrus leafminer mediated by a noncompetitive mechanism at a remarkably low pheromone release rate, J. Chem. Ecol. 34 (8) (2008) 1107–1113.
[10] B.G. Ambrogi, E.R. Lima, L. Sousa-Souto, Efficacy of mating disruption for control of the coffee leaf miner Leucoptera Coffeella (Guérin-Méneville) (Lepidoptera: Lyonetiidae), BioAssay 1 (8) (2006) 1–5.
[11] M. Michereff Filho, E.F. Vilela, G.N. Jham, A. Attygalle, A. Svatos, J. Meinwald, Initial studies of mating disruption of the tomato moth, Tuta absoluta (Lepidoptera: Gelechiidae) using synthetic sex pheromone, J. Braz. Chem. Soc. 11 (6) (2000) 621–628.
[12] M. di Bernardo, A.R. Champneys, C.J. Budd, P. Kowalczyk, Qualitative Theory of Non-Smooth Dynamical Systems, Springer London, London, 2008.
[13] M. di Bernardo, C.J. Budd, A.R. Champneys, P. Kowalczyk, A.B. Nordmark, G.O. Tost, P.T. Piiroinen, Bifurcations in nonsmooth dynamical systems, SIAM Rev. 50 (4) (2008) 629–701.
[14] H. Barclay, P. Van den Driessche, Pheromone trapping models for insect pest control, Res. Popul. Ecol. 25 (1) (1983) 105–115.
[15] H.J. Barclay, G.J. Judd, Models for mating disruption by means of pheromone for insect pest control, Res. Popul. Ecol. 37 (2) (1995) 239–247.
[16] M. Fisher, P. Van Den Driessche, H. Barclay, A density dependent model of pheromone trapping, Theor. Popul. Biol. 27 (1) (1985) 91–104.
[17] S. Ekesi, P. Nderitu, I. Rwomushana, Field infestation, life history and demographic parameters of the fruit fly Bactrocera invadens (Diptera: Tephritidae) in africa, Bull. Entomol. Res. 96 (04) (2006) 379–386.
[18] J. La Salle, The Stability of Dynamical Systems, Society for Industrial and Applied Mathematics, 1976.

[19] H.L. Smith, Monotone dynamical systems: an introduction to the theory of competitive and cooperative systems, Mathematical Surveys and Monographs, vol. 41, American Mathematical Society, 2008.
[20] R. Anguelov, Y. Dumont, J. Lubuma, Mathematical modeling of sterile insect technology for control of anopheles mosquito, Comput. Math. Appl. 64 (3) (2012) 374–389, doi:10.1016/j.camwa.2012.02.068.
[21] H.J. Barclay, J. Hendrichs, Models for assessing the male annihilation of Bactrocera spp. with methyl eugenol baits, Ann. Entomol. Soc. Am. 107 (1) (2014) 81–96.
[22] W. Walter, Differential and integral inequalities, vol. 55, Springer Science & Business Media, 2012.
[23] MATLAB, Version 7.14.0.739 (R2012a), The MathWorks Inc., Natick, Massachusetts, 2012.
[24] R.E. Bank, W.M. Coughran Jr, W. Fichtner, E.H. Grosse, D.J. Rose, R.K. Smith, Transient simulation of silicon devices and circuits, IEEE Trans. Comput.-Aided Des. Integr. Circuits Syst. 4 (4) (1985) 436–451.
[25] M. Hosea, L. Shampine, Analysis and implementation of TR-BDF2, Appl. Numer. Math. 20 (1) (1996) 21–37.
[26] T. Yamanaka, Mating disruption or mass trapping? numerical simulation analysis of a control strategy for lepidopteran pests, Popul. Ecol. 49 (1) (2007) 75–86.
[27] T. Yamanaka, S. Tatsuki, M. Shimada, An individual-based model for sex-pheromone-oriented flight patterns of male moths in a local area, Ecol. Model. 161 (1) (2003) 35–51.
[28] J.A. Byers, Simulation of mating disruption and mass trapping with competitive attraction and camouflage, Environ. Entomol. 36 (6) (2007) 1328–1338.
[29] C. Dufourd, C. Weldon, R. Anguelov, Y. Dumont, Parameter identification in population models for insects using trap data, BioMath 2 (2) (2013) 1312061.
[30] R. Anguelov, C. Dufourd, Y. Dumont, Simulations and parameter estimation of a trap-insect model using a finite element approach, Math. Comput. Simul. 133 (2017) 47–75.